ORGANIC LETTERS

2011
Vol. 13, No. 8
1948–1951

Semiconducting 2,6,9,10-Tetrakis(phenylethynyl)anthracene Derivatives: Effect of Substitution Positions on Molecular Energies

Jung A Hur†, Suk Young Bae, Kyung Hwan Kim, Tae Wan Lee, Min Ju Cho, and Dong Hoon Choi*

Department of Chemistry, College of Science, Research Institute for Natural Sciences, Korea University, 5 Anam-dong, Sungbuk-gu, Seoul 136-701, Korea

dhchoi8803@korea.ac.kr

Received January 31, 2011

ABSTRACT

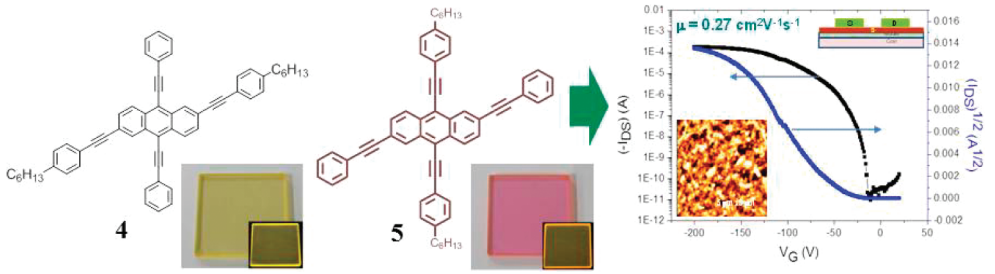

2,6-Bis((4-hexylphenyl)ethynyl)-9,10-bis(phenylethynyl)anthracene, 4, and 9,10-bis((4-hexylphenyl)ethynyl)-2,6-bis (phenyl ethynyl)anthracene, 5, have been synthesized to study their electronic and photophysical properties. It should be noted that the difference between these compounds is the substitution position of 1-ethynyl-4-hexylbenzene groups into an anthracene ring. In particular, substitution in the 9,10-positions of the anthracene ring enhanced J-aggregated intermolecular interactions. Since 5 has a lower bandgap energy and more compact film morphology, it exhibited higher hole mobility (~0.27 $cm^2 V^{-1} s^{-1}$) in thin-film transistor devices.

Because of recent rapid progress in the development of novel p-type organic semiconductors, derivatives of pentacene, rubrene, anthracene, and thiophene have attracted attention because of their applications in high-performance organic thin-film transistors (OTFTs).[1−5] Research has focused on replacing vacuum-processable materials with solution-processable materials to overcome severe limitations in large-scale device fabrication due to the complexity of the process.[6−10] Two-dimensional π-extended conjugated molecular structures have shown effective charge-transport properties as films, satisfying the requirements for soluble semiconducting materials.[11,12] It is well recognized that electronic structure, molecular structure, and morphology of thin films are important for enhancing carrier mobility in TFT devices. With respect to "electronic structure," small bandgap energy, large bandwidth, small ionization potential, and large π-conjugation

(1) (a) Nelson, S. F.; Lin, Y.-Y.; Gundlach, D. J.; Jackson, T. N. *Appl. Phys. Lett.* **1998**, *72*, 1854–1856. (b) Zheng, Q.; Chen, S.; Zhang, B.; Wang, L.; Tang, C.; Katz, H. E. *Org. Lett.* **2011**, *13*, 324–327.

(2) (a) Lee, W. H.; Kim, D. H.; Cho, J. H.; Jang, Y.; Lim, J. A.; Kwak, D.; Cho, K. W. *Appl. Phys. Lett.* **2007**, *91*, 092105. (b) Liu, W. J.; Zhou, Y.; Ma, Y.; Cao, Y.; Wang, J.; Pei, J. *Org. Lett.* **2007**, *9*, 4187–4190.

(3) (a) Briseno, A. L.; Tseng, R. J.; Ling, M. −M.; Falcao, E. H. L.; Yang, Y.; Wudl, F.; Bao, Z. *Adv. Mater.* **2006**, *18*, 2320–2324. (b) Chuang, T. H.; Hsieh, H. H.; Chen, C. K.; Wu, C. C.; Lin, C. C.; Chou, P. T.; Chao, T. H.; Chow, T. J. *Org. Lett.* **2008**, *10*, 2869–2872.

(4) Zhang, L.; Tan, L.; Wang, Z.; Hu, W.; Zhu, D. *Chem. Mater.* **2009**, *21*, 1993–1999.

(5) Gao, P.; Beckmann, D.; Tsao, H. N.; Feng, X.; Enkelmann, V.; Baumgarten, M.; Pisula, W.; Müllen, K. *Adv. Mater.* **2009**, *21*, 213–216.

(6) Silvestri, F.; Marrocchi, A.; Seri, M.; Kim, C.; Marks, T. J.; Facchetti, A.; Taticchi, A. *J. Am. Chem. Soc.* **2010**, *132*, 6108–6123.

(7) Park, S. K.; Jackson, T. N.; Anthony, J. E.; Mourey, D. A. *Appl. Phys. Lett.* **2007**, *91*, 063514.

(8) Gundlach, D. J.; Royer, J. E.; Park, S. K.; Subramanian, S.; Jurchescu, O. D.; Hamadani, B. H.; Moad, A. J.; Kline, R. J.; Teague, L. C.; Kirillov, O.; Richter, C. A.; Kushmerick, J. G.; Richter, L. J.; Parkin, S. R.; Jackson, T. N.; Anthony, J. E. *Nat. Mater.* **2008**, *7*, 216–221.

(9) Fong, H. H.; Pozdin, V. A.; Amassian, A.; Malliaras, G. G.; Smilgies, D. −M.; He, M.; Gasper, S.; Zhang, F.; Sorensen, M. *J. Am. Chem. Soc.* **2008**, *130*, 13202–13203.

10.1021/ol200299s
Published on Web 03/16/2011

length are essential requirements for designing high-mobility semiconducting molecules. To steer the bandgap energy and molecular energy levels, such as the highest occupied molecular orbital (HOMO) and the lowest unoccupied molecular orbital (LUMO) energies, varying the conjugation length of a molecule or introducing donor/acceptors into the π-conjugated molecular frames are often adopted for designing new semiconducting materials, which is the basis of "molecular structure". Instead of changing the entire molecular structure, it is preferable to use a method capable of changing the molecular energies in a film only by changing the position of alkyl substituents (e.g., solubilizing groups) while maintaining an identical π-conjugated molecular skeleton. Even if the electronic and photophysical properties of solutions of two different molecules are identical, their solid states can exhibit different properties, which is the basis of "crystalline morphologhy."

In this paper, we present one interesting π-conjugated core unit, 2,6,9,10-tetrakis(phenylethynyl)anthracene. Our molecular design principle is to vary the substitution positions of 1-ethynyl-4-hexylbenzene groups in an anthracene ring. We tethered two 1-ethynyl-4-hexylbenzene groups into 2,6-positions for **4** and into 9,10-positions for **5**. We show that the hexyl side group enhances not only the solubility but also the degree of self-organization (i.e., molecular ordering). The facile and high-yield synthesis of two new p-type anthracene-based semiconducting molecules is reported in this work. Scheme 1 illustrates the synthetic routes for the two molecules.

New anthracene-containing π-conjugated molecules have been synthesized using reduction and Sonogashira coupling reactions. Ethynylbenzene was synthesized following the literature method.[13] 2,6-Dibromoanthracene-9,10-dione was also synthesized according to an established method.[14,15] Addition of the dione compound to 2 molar equiv of 1-ethynyl-4-hexylbenzene in the presence of bis(triphenylphosphine)palladium(II) dichloride and copper iodide afforded **1**. The reduction reaction using tin chloride in an acidic medium gave the desired compound, **2**.[16] For preparation of **4**, 2,6-bis((4-hexylphenyl)ethynyl) anthracene-9,10-dione was also used to anchor the ethynylbenzene through reduction, similar to the method for **2**. Sonogashira coupling reactions were performed, providing **5** in a 47% yield.

Scheme 1. Synthesis of 2,6,9,10-Tetrakis(phenylethynyl) anthracene Derivatives

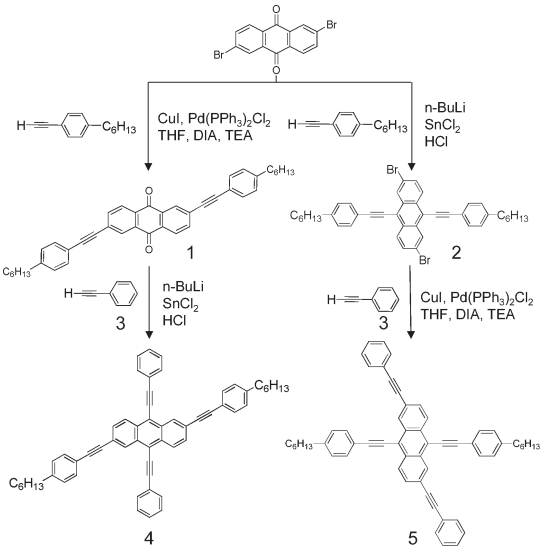

It should be noted that 2,6,9,10-tetrakis(phenylethynyl) anthracene is not soluble in common organic solvents. After tethering hexyl chains to phenyl rings, the molecules showed good solubility (10 mg/1 mL of $CHCl_3$ for **4** and **5**). The identity and purity of the synthetic materials were confirmed by ^{1}H NMR, ^{13}C NMR, HRMS, and elemental analysis (see the Supporting Information).

Recently, we reported the facile synthesis of 5,5′-((9,10-bis((4-hexylphenyl)ethynyl)anthracene-2,6-diyl)bis-(ethyne-2,1-diyl))bis(2-hexylthiophene), which exhibited superior p-type semiconducting behavior evidenced by very high carrier mobility in a TFT device.[16] However, the origin of strong intermolecular interactions in film form was ambiguous. Therefore, the common phenylethynyl groups in four positions were introduced into the anthracene ring, and then,we varied two substitution positions of 1-ethynyl-4-hexylbenzene in the ring.

The thermal properties of the molecules were characterized by differential scanning calorimetry (DSC) and thermogravimetric analysis (TGA). DSC measurements were performed under nitrogen with the highest temperature limited to below the decomposition temperature. Molecules **4** and **5** exhibited distinct crystalline-isotropic transition temperatures of 183 and 223 °C and cold crystallization temperatures (T_ms) of 154 and 127 °C, respectively (see Figure 1S, Supporting Information). Comparison showed that the presence of two 1-ethynyl-4-hexylbenzene peripheral groups at the 9,10-positions of the anthracene ring induced higher T_m, suggesting that a stronger intermolecular interaction exists for the denser molecular packing along the 9,10-directions in **5**. TGA measurements revealed that the molecules had almost identical, good thermal stabilities (T_d's of **4** and **5** = 428 °C, see Figure 2S, Supporting Information).

We hypothesized that the two peripheral hexyl groups in **4** and **5** gave rise to high crystallinity due to the tight

(10) Tang, M. L.; Reichardt, A. D.; Miyaki, N.; Stoltenberg, R. M.; Bao, Z. *J. Am. Chem. Soc.* **2008**, *130*, 6064–6065.
(11) (a) Li, H.; Valiyaveettil, S. *Tetrahedron Lett.* **2009**, *50*, 5311–5314. (b) Wang, C.; Liu, Y.; Ji, Z.; Wang, E.; Li, R.; Jiang, H.; Tang, Q.; Li, H.; Hu, W. *Chem. Mater.* **2009**, *21*, 2840–2845.
(12) (a) Hoang, M. H; Cho, M. J.; Kim, K. H.; Lee, T. W.; Jin, J. I.; Choi, D. H. *Chem. Lett.* **2010**, *39*, 396–397. (b) Pisula, W.; Menon, A.; Stepputat, M.; Lieberwirth, I.; Kolb, U.; Tracz, A.; Sirringhaus, H.; Pakula, T.; Müllen, K. *Adv. Mater.* **2005**, *17*, 684–689.
(13) Okutani, M.; Mori, Y. *J. Org. Chem.* **2009**, *74*, 442–444.
(14) Hodge, P.; Power, G. A.; Rabjohns, M. A. *Chem. Commun.* **1997**, 73–74.
(15) Zhang, H. C.; Guo, E. Q.; Zhang, Y. L.; Ren, P. H.; Yang, W. J. *Chem. Mater.* **2009**, *21*, 5125–5135.
(16) Jung, K. H.; Bae, S. Y.; Kim, K. H.; Cho, M. J.; Lee, K.; Kim, Z. H.; Choi, D. H.; Lee, D. H.; Chung, D. S.; Park, C. E. *Chem. Commun.* **2009**, *35*, 5290–5292.

Table 1. Measured and Calculated Parameters of Molecules **4** and **5**

molecule	T_m (°C)	T_d (°C)	$\lambda_{max}^{abs a}$ (nm)	$\lambda_{max}^{PL a}$ (nm)	$\lambda_{max}^{abs b}$ (nm)	$\lambda_{max}^{PL b}$ (nm)	HOMO[c] (eV)	LUMO[d] (eV)	E_g^{opte}(eV)
4	183	429	430, 459, 486	506, 539	448, 473, 510	525, 563	−5.78	−3.44	2.34
5	223	427	430, 466, 486	513, 543	468, 499, 540	557, 592	−5.73	−3.52	2.21

[a] Measured in chloroform with a concentration of 10^{-5} M. [b] Films were spin-coated from chloroform solution. [c] The values were obtained from cyclic voltammograms. *Sample: film on Pt electrode. [d] HOMO (eV) − E_g^{opt} (eV). [e] The optical bandgaps were obtained from absorption spectra of film samples.

packing of molecules along the lateral directions and, hence, may enhance carrier-transport properties in TFT devices.

To study intermolecular interactions between the molecules, absorption spectra of the samples in chloroform (conc 1 $\times 10^{-6}$ mol/L) and were obtained as thin films (Figure 1 and Table 1).

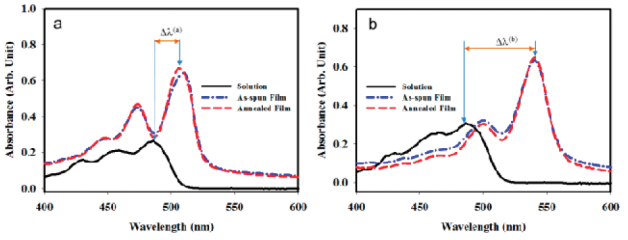

Figure 1. UV−vis absorption spectra of solution (−), as-spun film (--), and thermally annealed film (-·-): (a) **4**, (b) **5**. $\Delta\lambda^{(a)}$ = 17 nm, $\Delta\lambda^{(b)}$ = 54 nm.

In **4** and **5**, we observed a significant bathochromic shift in the absorption spectra upon film formation, indicating the generation of strong intermolecular interactions. In contrast to the solution phase spectra, the spectra of the two molecules as spin-cast films were more structured. Comparing the wavelength shift from the absorption maxima in solution and annealed film spectra indicated that molecules of **5** are subject to stronger intermolecular interactions in the solid state.

Compared with **4** ($\Delta\lambda^{(a)}$ = 17 nm), **5** exhibited a larger bathochromic shift, ($\Delta\lambda^{(b)}$ = 54 nm), implying that a higher degree of J-aggregation exists in the films.[17−19] The optical bandgap (E_g^{opt}) of **5** is 2.21 eV, which is smaller than that of **4** (E_g^{opt} = 2.34 eV). Switching the substitution positions of 1-ethynyl-4-hexylbenzene from the 2,6- to 9,10-positions caused the bandgap to decrease in the solid state, although the solution state gave identical bandgap energies (E_g^{opt} = 2.44 eVz).

Importantly, no thermal annealing effect was observed in film samples of the two molecules, implying that the films were fully comprised of polycrystalline domains that were preorganized after spin-coating.

Figure 2 shows emission spectra of the two molecules with identical skeletons under an excitation wavelength of 370 nm. For **4**, the emission spectrum of the thermal annealed film was more structured than that of the as-spun film, while no annealing effect was observed in the film spectra of **5**. The emission bands of **5** appeared at longer wavelengths than those of **4**, which is consistent with the results of absorption spectral analysis. For instance, a nonaggregated emission band appeared at 557 nm, and the emission band at 592 nm can be assigned to the J-aggregated characteristic band. In particular, we acquired the emission spectra of single crystals, which displayed longer emission bands compared with those of solutions and films. The fluorescence lifetimes obtained from time-correlated single-photon-counting measurement can support the above explanation (see Figures 6S and 7S, Supporting Information). The emission band in **5** was slightly longer than that in **4**, indicating formation of more highly ordered structures in the crystalline morphology.

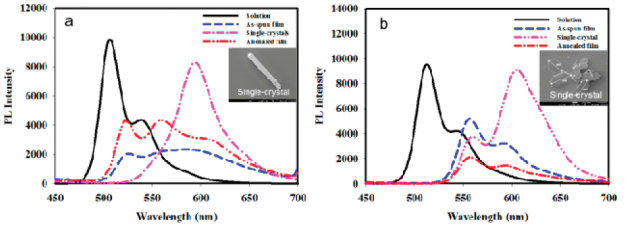

Figure 2. Photoluminescence (PL) spectra of **4** (a) and **5** (b): solution spectra (−); as-spun film (--); single crystals (-·-); thermally annealed film (-···-). *Single crystals were grown via solvent slow diffusion methods at 25 °C (THF/MeOH = 1:3 v/v).

To elucidate the HOMO and LUMO energy levels of these molecules, their electrochemical properties were investigated by cyclic voltammetry. Cyclic voltammograms (CV) were recorded on a film sample, and the potentials were obtained relative to an internal ferrocene reference (Fc/Fc^+). These CV scans in the range of −1.5 V to +1.5 V (vs Ag/AgCl) show quasi-reversible oxidation peaks. Unfortunately, the reduction behaviors were irreversible; therefore, we were unable to accurately estimate their HOMO and LUMO energies.

To determine the LUMO levels, we combined the oxidation potential in CV with the optical energy bandgap (E_g^{opt}) resulting from the absorption edge in the absorption spectrum. Voltammograms of **4** and **5** in film form show that their lowest oxidative waves commonly occur around 1.38 and 1.33 V (E_{ox}^{onset} = +1.09 V for **4** and **5** solutions). As shown in Table 1, the films have HOMO

levels of −5.78 eV for **4** and −5.73 eV for **5**. In addition, **4** and **5** have LUMO energy levels of around −3.44 and −3.52 eV. Results from CV analyses of films confirmed the effect of substitution position on the molecular energy level.

Bottom-gate top-contact OTFT devices were fabricated under ambient conditions without thermal annealing, and gold source and drain electrodes were thermally evaporated using the conventional method.[20] A 400-nm thin film of the semiconductor was deposited by spin-coating a 1 wt % solution of the molecules in chloroform without thermal annealing. The channel length was $L = 100\ \mu$m, and the channel width was $W = 1500\ \mu$m. Devices I and II contained semiconducting layers of **4** and **5**, respectively.

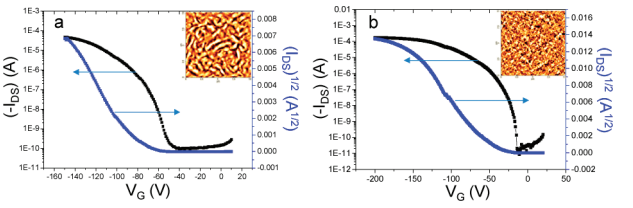

Figure 3. Transfer characteristics of two OTFT devices: (a) device I, (b) device II. *Insulator: *n*-octyltrichlorosilane (OTS)-treated SiO_2 *Inset: atomic force microscopy (AFM) images of the prestine film in TFT devices.

The OTFTs of the molecules exhibited typical p-channel field-effect transistor (FET) characteristics (Figure 3). The output characteristics showed very good saturation behaviors and clear saturation currents that were quadratic to the gate bias. The mobilities were obtained from the source (S)−drain (D) current−voltage curves (I_{DS} vs V_{DS}) in well-resolved saturation regions. The mobility of device II (μ = 0.27 $cm^2\ V^{-1}\ s^{-1}$; μ_{max} = 0.30 $cm^2\ V^{-1}\ s^{-1}$) was higher than that of device I (μ = 0.17 $cm^2\ V^{-1}\ s^{-1}$). Interesting properties of the devices include very high on/off current ratios ($I_{on/off} = 10^6-10^7$). In device II, $I_{on/off} > 10^7$ indicates that the device was well fabricated, having great interfacial contact and limited leakage current. Note that carrier mobilities larger than 0.1 $cm^2\ V^{-1}\ s^{-1}$ have rarely been achieved in devices of as-spun films of organic semiconducting molecules. The significantly large mobility of device II is mainly attributable to the high degree of microstructural order of grains as well as the two-dimensional molecular arrangement within grains associated with the molecular structure of two hexyl peripheral groups.

In conclusion, we successfully synthesized and characterized new anthracene-based conjugated molecules that are solution processable. Depending on the substitution positions of 1-ethynyl-4-hexylbenzene, the molecular energy levels and bandgap energies were tuned. Molecule **5**, bearing 1-ethynyl-4-hexylbenzene subsitituents at the 9,10-positions in the anthracene ring, showed a much smaller bandgap energy in film form, although the two molecules are identical in the solution phase. Remarkably, the device bearing the as-spun film of **5** showed greater enhancement of carrier mobility, indicating that the uniform lamella and π-stacking of molecule **5** facilitates carrier transport more effectively.

Our study unambiguously demonstrates that molecular energy levels, including optical and photophysical properties of films, can be modulated only by changing the substitution positions with alkyl chains, although the central conjugated molecular skeletons are identical.

Acknowledgment. This research was supported by Korea Science and Engineering (KOSEF R012007000-1128402008) and by the Priority Research Centers Program through the National Research Foundation of Korea (NRF) funded by the Ministry of Education, Science and Technology (NRF20100020209).

Supporting Information Available. Experimental procedures and full characterizations data. Fabrication of TFT devices, results of DFT calculations, thermal analysis data, lifetime measurements, NMR spectra of **4** and **5** etc. This material is available free of charge via Internet at http://pubs.acs.org.

(17) Chan, J. M. W.; Tischler, J. R.; Kooi, S. E.; Bulović, V.; Swager, T. M. *J. Am. Chem. Soc.* **2009**, *131*, 5659–5666.
(18) Walker, B. J.; Bulović, V.; Bawendi, M. G. *Nano Lett.* **2010**, *10*, 3995–3999.
(19) Möbius, D. *Adv. Mater.* **1995**, *7*, 437–444.
(20) Park, J. H.; Chung, D. S.; Park, J. W.; Ahn, T.; Kong, H.; Jung, Y. K.; Lee, J.; Yi, M. H.; Park, C. E.; Kwon, S. K.; Shim, H. K. *Org. Lett.* **2007**, *9*, 2573–2576.